Modelling of HVDC breakers for HVDC grid simulations

T Augustin[*], *S Norrga*[*], *H-P Nee*[*]

[*]*KTH Stockholm, Sweden, timau@kth.se*

Keywords: HVDC, HVDC breaker, HVDC grid, PSCAD

Abstract

This paper deals with the modelling of high-voltage direct current (HVDC) breakers in PSCAD. The models are aimed at HVDC grid simulation and are kept as simple as possible. An overview is given over recently proposed HVDC breaker concepts. Assumptions and simplifications are explained as well. The main result is that even these simplified models are too detailed for grid simulations. The reason for this is that from a grid perpective the only thing that matters is when the metal-oxide varistor is inserted. The models can be used to estimate interruption times.

1 Introduction

High-voltage direct current (HVDC) grids have widely been accepted as a solution for a more sustainable electrical energy supply, because HVDC grids allow for large-scale integration of remote renewable energy resources. HVDC breakers are the missing element for future HVDC grids [1]. Several HVDC breaker concepts have been proposed in the literature. Before the forming of HVDC grids, further analysis of the HVDC breakers and their grid interaction is required.

This paper gives an overview of the existing HVDC breaker concepts. The breakers have been modelled in the simulation package PSCAD. The models are intended for HVDC grid simulations for instance based on the test grid described in [2]. Thus, higher-level models have been implemented to keep computation times short.

2 Overview of HVDC breakers

Several HVDC breaker concepts have been proposed in the literature. A good overview is given in [3]. The following section gives short descriptions of the most prospective recent ones, which we also modelled. The breakers all have a similar structure to the one shown in Fig. 1. For some concepts, the paths are connected differently. However, the operation sequence stays the same. The breaker current is flowing in the main path in normal operation. When the breaker is tripped, the current is commutated to the commutation path. The energy absorption path is needed to dissipate the stored system energy before interruption. Typically, metal-oxide varistors (MOV) with a nonlinear u-i characteristics are employed. When the breaker's voltage drop reaches the MOV clipping voltage, the MOV starts to conduct and inserts a counter-voltage. This counter-voltage opposes the system voltage and drives the fault current to zero.

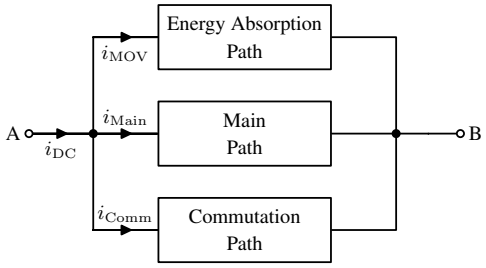

Fig. 1: General structure HVDC breaker

2.1 Active resonant breaker

The active resonant breaker is depicted in Fig. 2. When the breaker is tripped, the contacts of the mechanical breaker part and draw an arc. When the contact gap reaches sufficient seperation, the switch in the commutation path is triggered. This discharges the pre-charged capacitor and the injected current leads to a current zero in the main path. The arc extinguishes and the fault current commutates into the commutation path, charging the capacitor until the MOV starts to conduct.

This old concept was already described in [4] in the 70s. Mitsubishi Electric is currently promoting their version [5]. Vacuum interrupters are preferred as mechanical breakers due to the short required contact gap and light contacts allowing for fast seperation. Vacuum interrupters are available for $40.5\,\mathrm{kV}$. Thus, several breaks have to be connected in series with appropriate grading to ensure equal voltage distribution. A charging circuit is needed for the capacitor. As discharge switch a triggered spark-gap or thyristors could be used. With the latter option, many series-connected devices would be required. In our models, we have assumed a spark-gap. If bidirectional breaking is needed, one can discharge the capacitor as usual and wait for the second half-wave of the oscillating pulse current. Otherwise, the capacitor voltage has to be reversed with extra circuitry, see for instance [6]. We have modelled the prior option. Also, we included a back-up capacitor in the model with its own discharge switch. In the simulation, the inductor was chosen as $10\,\mathrm{mH}$ and the capacitor as $10\,\mu\mathrm{F}$.

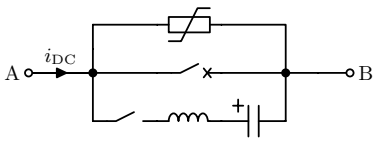

Fig. 2: Active resonant HVDC breaker

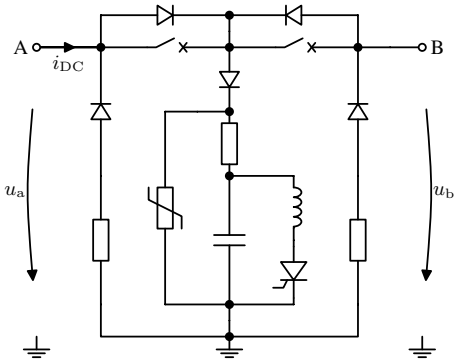

Fig. 3: HVDC breaker proposed by Wang & Marquardt

2.2 Wang & Marquardt breaker

Wang & Marquardt introduced a concept in [7], which has some similarities with active resonant breakers, see Fig. 3. The capacitor is charged from the line voltage through the pulse generator diode, so that no charging circuit is required. When the breaker is tripped, the contacts of both switches part. The arc voltage commutates the current from the switch on the side away from the fault to its parallel diode. When the contact gap is sufficient the thyristor is triggered. This causes a current pulse which reverses the capacitor voltage. When the capacitor voltage becomes negative, the diodes in the adjacent branches conduct. The pulse current creates a current zero in the arcing switch on the fault-side. Current superposition in the diode away from the fault-side leads to large current stress. The fault current commutates to the pulse generator branch and recharges the capacitor until the MOV starts to conduct.

Vacuum interrupters are used as mechanical breakers. It is also possible to leave the elements left of the pulse generator out, if only unidirectional breaking is required. For the simulations, we have included a back-up pulse generator in parallel to the mentioned one. In the simulation, the resistor, inductance, and capacitor in the pulse generator were chosen as $10\,\Omega$, $0.1\,\mathrm{mH}$, and $10\,\mu\mathrm{F}$, respectively. The resistor in the damping branch was set to $0.05\,\Omega$.

2.3 ABB hybrid breaker

ABB described their concept in [8], see Fig. 4. It uses a disconnector and an IGBT stack in its main path. The IGBT stack in the main path is named load commutation switch (LCS). The commutation path consists of IGBT stacks, each in parallel with an MOV. When I_{DC} rises beyond a current threshold, the LCS is turned off and the IGBT stacks in the commutation path turn on. The current commutates to the commutation path. This is done before the actual tripping. ABB calls this *proactive tripping* and we adopt this terminology. The disconnector starts opening without arcing, which takes approx. $2\,\mathrm{ms}$. If the breaker is tripped or the current passes the maximum permissible value, the IGBTs in the commutation path are turned off, diverting the current into the MOV. An overcurrent limitation mode is also described in this paper. Here, not all stacks in the commutation path are turned off at once, but instead successively in such a fashion, that the fault current is limited.

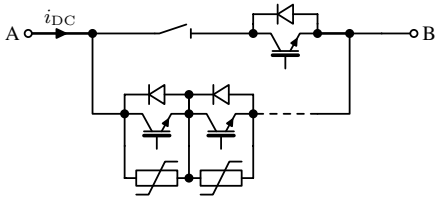

Fig. 4: ABB hybrid HVDC breaker

ABB uses an SF6-based disconnector [9]. The LCS only has to be dimensioned for a low voltage, the on-state voltage drop of the IGBTs in the commutation path. Thus, only a few IGBT positions are needed for the LCS. In [10], the LCS is described in detail. It is also possible to use this concept with an arcing mechanical breaker and without LCS. In this case, the arc voltage transfers the current to the commutation path. In [11], SF6 and vacuum interrupters are compared. The results showed that the metal-vapor arc voltage is too low to completely commutate the current. However, SF6 interrupters require a rather long time to open. If bidirectional breaking is needed, stacks have to be connected in antiparallel, doubling the semiconductor expenditure.

2.4 Alstom hybrid breaker

Alstom presented their hybrid breaker concept in [12], see Fig. 5. The main path is the same as for the ABB concept. However, Alstom replaced the IGBTs in the commutation path by three thyristor branches. To commutate the current out of the main path, the LCS is turned off and the thyristor in the first branch is fired. When the current has commutated, the disconnector opens. The fault current charges the capacitor in the first branch until the MOV limits the voltage. This MOV voltage is in the order of the LCS rated voltage. The thyristor in the second branch is fired and the current commutates to this branch. The MOV voltage in the second branch is slightly higher than the one in the first branch. Both capacitors are dimensioned so that the disconnector has opened sufficiently when the capacitors are charged. The thyristors in the third branch are fired when the breaker is tripped. Finally, the current commutates to the energy absorption path.

If additional time-delays are required, more thyristor branches could be added. This could be used to achieve fault-current

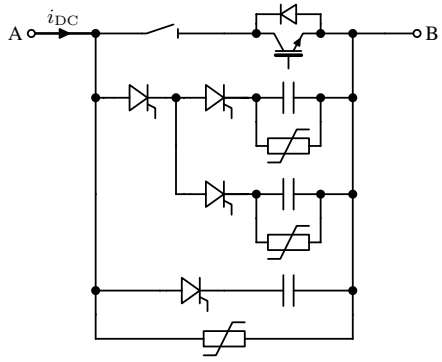

Fig. 5: Alstom hybrid HVDC breaker

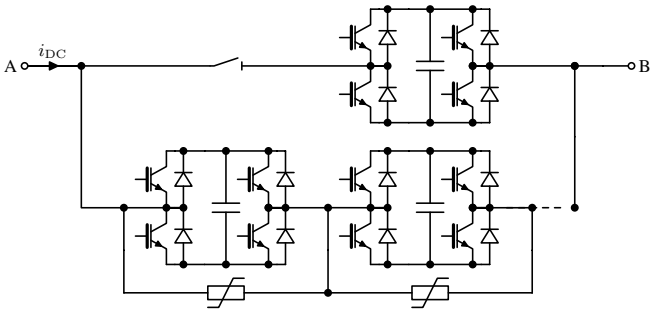

Fig. 6: SGCC hybrid HVDC breaker

limitation. For bidirectional breaking, thyristors have to be installed in antiparallel. Before the breaker can operate again after an interruption, the capacitors have to be discharged. This has not been described in the above-referenced paper. In the simulation, the capacitors from the top to the bottom were set to the following values: $1\,\mathrm{mF}$, $0.1\,\mathrm{mF}$ and $1\,\mu\mathrm{F}$.

2.5 SGCC hybrid breaker

State Grid Corporation of China (SGCC) introduced the concept shown in Fig. 6 [13]. This concept is very similar to the ABB concept. Full-bridges replace the IGBT stacks and are used as LCS as well. The operation sequence is the same as for the ABB concept. The current in a conducting full-bridge splits in two branches each consisting of an IGBT and a body diode. The main difference to the ABB concept is that if a full-bridge is turned off, the capacitor is inserted in the path by two conducting body diodes. The current commutates, if all inserted capacitors in a path are sufficiently charged. Due to the full-bridges, the SGCC concept can break bidirectionally. This concept uses vacuum interrupters as disconnectors. In the simulation, the full-bridge capacitances were set to $1\,\mu\mathrm{F}$.

3 Modelling

The models should be simple for reasonable simulation times. The chosen simplifications, which are common for all developed models, are described in the following. Also, a test grid for the simulation is explained.

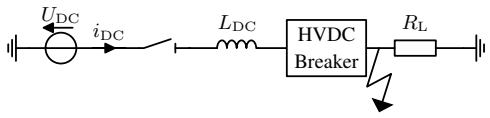

Fig. 7: Test grid for simulation with $U_{\mathrm{DC}} = 320\,\mathrm{kV}$, $L_{\mathrm{DC}} = 100\,\mathrm{mH}$ and $R_{\mathrm{L}} = 200\,\Omega$

3.1 Test grid

The grid used to test the models is shown in Fig. 7. The voltage source U_{DC} models the converter voltage. The disconnector is needed to interrupt residual currents. The inductor L_{DC} limits the slope of the fault current. To get the pre-fault load current, a passive resistive load is used. A control block, which is not shown in the figure, is used to model different operating scenarios. The ones we considered are close-open-reclose, arc re-ignition, overcurrent limitation, and initial faults on the bus-bar.

3.2 Simplifications

An important question is, which elements could be neglected. If one approximates the stray inductance as a square coil with side length $l = 10\,\mathrm{m}$ and round conductor cross-section with radius $R = 2\,\mathrm{cm}$, the formula

$$L_{\mathrm{stray}} = \frac{2\mu_0 l}{\pi}\left(\log\left(\frac{2l}{R}\right) + \sqrt{2} - \operatorname{asinh}(1) - 1.75\right) \quad (1)$$

from [14] with the vacuum permeability μ_0 yields $45\,\mu\mathrm{H}$. A test simulation with this stray inductance between the main and commutation path showed no significant impact for the modelled breakers. However, if arcing is actively used to commutate the current as done in the ABB breaker without LCS, the stray inductance should be considered.

Snubber circuits have not been depicted in the above-shown HVDC breaker schematic diagrams, but all semiconductor-based concepts need snubbers. Snubbers are regarded as unnessary details for our models, because they will mainly just introduce small time delays, for instance for commutation. Thus, snubbers have been omitted. However, this leads to numerical problems and warnings in PSCAD in some cases. To solve this, a very small simulation capacitor with $1\,\mathrm{pF}$ has been connected across the semiconductor-based breakers. Choosing the smallest possible capacitor assures that the accuracy of the models is not impaired, while still getting rid of numerical problems.

3.3 Flexiblity

The models should be flexible with regards to the ratings and the circuit configuration. This means that, for instance, the ABB breaker could have a different number of stacks in the

commutation path depending on the voltage level. PSCAD offers two possibilities to create custom models: Modules and components. Modules consist of a canvas, on which circuit elements can be placed. This is not flexible. On the other hand, components are created with special statements in the respective segments. Here, conditional statements can be used to configure the circuit according to user input. The circuit is defined in the Branch segment. Unfortunately, no loop-directive is available in PSCAD. Instead, #IF-directives can be added and duplicated to build a circuit with a predefined maximum of repeated circuit structures. Also, internal multidimensional-nodes can be added in the Graphics section and Fortran code in the DSDYN segment to define the breaker and its operation. Note that we have used conventional modules for the active resonant breaker and Marquardt's concept, because they do not feature repeated elements. The hybrid breakers are realized as modules as well, but the elements inside, such as the disconnector, the LCS, and the commutation path, as individual components. This way the building blocks can be reused in similar concepts. Also, the breaker control block has been implemented as component for each concept. This facilitates code reuse and also proved less prone to errors than manually configuring logic blocks.

3.4 Arcing

Arcing has been considered with a black-box-model. In [15], the Cassie-like model

$$\frac{\mathrm{d}g_{\mathrm{arc}}}{\mathrm{d}t} = \frac{1}{\tau_0}\left(\frac{u_{\mathrm{arc}}^2 g_{\mathrm{arc}}^{1.4}}{P_0} - g_{\mathrm{arc}}\right) \tag{2}$$

with the arc conductance g_{arc}, the arc time constant τ_0, the cooling power P_0, and the arc voltage u_{arc} is used to analyze dc arcs. In that paper, the authors analyzed passive resonant breakers and also neglected the time derivative and linearized the nonlinear conductance due to the slow arc changes. However, we had problems with these assumptions in our simulations. The fault current increases fast in general and with a static nonlinear u-i characteristic the arc voltage drops so fast that the current does not commutate out of the main path. Thus, we used (2) as it is, solved it and took the inverse to get the arc resistance. The values $P_0 = 4.25 \times 10^6\,\mathrm{V}^{1.6}\,\mathrm{A}^{0.4}$ and $\tau_0 = 4\,\mu\mathrm{s}$ are taken from [16] for a $362\,\mathrm{kV}$ breaker. Vacuum arcs are much more difficult to model and nothing applicable has been published. Thus, we used the same values as above.

3.5 Disconnector

The disconnectors have been modelled as ideal single-phase breakers, which are allowed to open after a delay time, if the current is smaller than a residual current, as proposed in [10].

3.6 Series and parallel connected semiconductors

Semiconductor valves consisting of M-series- and N-parallel connected semiconductors, which are switched simultaneously, can be modelled as one equivalent semiconductor with adapted on- and off-state resistance. The values have to be multiplied by M/N. The series-connected full-bridges in the SGCC breaker are lumped together in the same way.

One thing to note is that the actual values of on- and off-state resistances are not important for the kind of modelling used, unless arcing is used to commutate currents. Looking at Fig. 1, one branch has a very high resistance and the other one a very low in the commutation process. Thus, the commutation is not influenced as long as the relation between on and off is right. Therefore, we used typical PSCAD values such as $1\,\mathrm{m\Omega}$ for the on-resistance and $1\,\mathrm{M\Omega}$ for the off-resistance for a semiconductor stack. If arcing is used to commutate the current, as in the ABB-concept without LCS, this should not be done. The arcing voltage is in the same range as the total on-state voltage drop of the semiconductors, so that the number of semiconductors and their characteristics have a significant impact on commutation. Here, we assumed four stacks with each 40 IGBTs in series. Furthermore, we assumed ABB's $4.5\,\mathrm{kV}$-IGBT-module 5SNA 1200G450300 with an on-state resistance of $2.2\,\mathrm{m\Omega}$ and an off-state resistance of $37.5\,\mathrm{k\Omega}$ for the IGBT and $1.9\,\mathrm{m\Omega}$ and $97.8\,\mathrm{k\Omega}$ for the diode, respectively.

3.7 Charging circuit

Charging circuits for pre-charged capacitors have been modelled as ideal single-phase dc voltages with series-connected resistors and single-phase breakers. The resistance value has to be chosen according to the expected charging time constant. The single-phase breaker is controlled with the possibility to open without a current zero-crossing.

Note that Marquardt's concept does not require a charging circuit at grid voltage level. For lower voltages, as used in the experiments reported in [7], the pulse current would be too low so that the capacitor has to be charged above the test voltage. We observed in our simulations that when charging from the line the capacitor was always charged higher than the line voltage. This can be understood by looking at the two existing RLC-circuits in Fig. 3. The pulse generator is dimensioned to give a pulse, hence an undamped oscillation. When charging the capacitor from the line, the grid inductance is part of the resonance circuit, but the resistance in the pulse branch is still determining the damping. Thus, overvoltages occur when charging from the line. The diode in the pulse branch rectifies the pulsating charging current leading to a capacitor voltage that is higher than the line voltage. It is questionable whether such a high voltage is beneficial. Higher voltages imply higher costs for components and insulation. It would be possible to use an MOV with lower clipping voltage, but this would also increase the interruption time. Instead, a charging resistor could be used in series with the pulse resistor to increase the damping. When the capacitor is charged, the charging resistor is short-circuited. We have done this in the simulation and used $300\,\Omega$ resistances in both pulse generators. Note that the resistance has to be adapted to the number of parallel pulse generators.

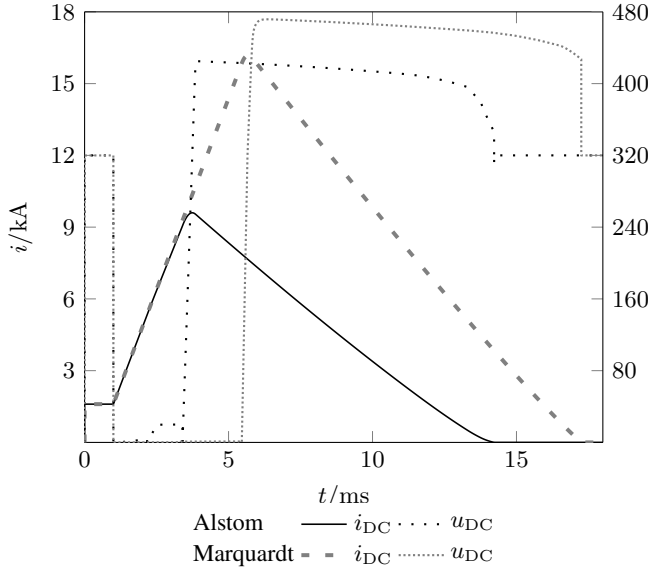

Fig. 8: Breaker current and voltage for Alstom and Marquardt HVDC breakers

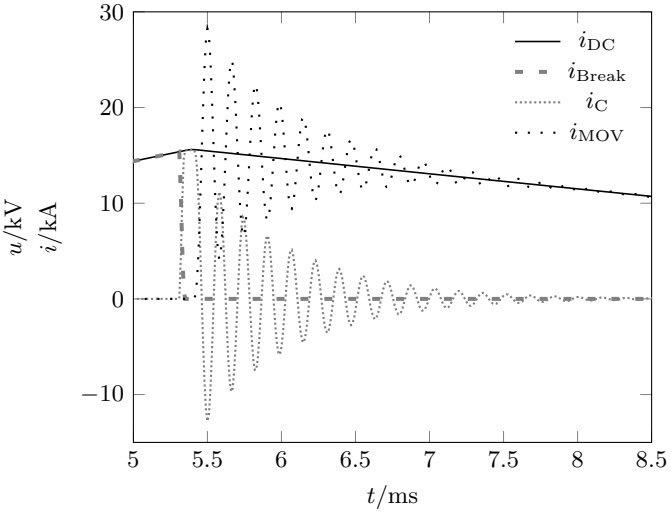

Fig. 9: Currents in active resonant breaker during commutation processes

4 Results & Discussion

The simulations were carried out with a load current of $1.6\,\mathrm{kA}$. The proactive trip level is set to $2\,\mathrm{kA}$ and the trip level to $9\,\mathrm{kA}$. The energy absorption MOV's total clipping voltage is set to $1.5U_{\mathrm{DC}} = 480\,\mathrm{kV}$. A fault is inserted after $1\,\mathrm{ms}$.

Fig. 8 shows the breaker current and voltage for the Alstom and Marquardt concepts. When the fault occurs, the breaker currents increase linearly due to the large dc inductor. For the Alstom breaker, the MOV starts inserting a voltage shortly after the trip, because the current was already in the commutation path due to the proactive tripping. The Marquardt breaker does not have this feature, so that $2\,\mathrm{ms}$ pass until the interrupters have opened and the commutation sequence starts. In both cases, the MOV's counter-voltage decreases the current linearly. The voltage curves also look similar, but for the Marquardt breaker the inserted voltage is higher due to the higher current. The plot shows that seen from the grid the only thing that matters is when the MOV starts to conduct. Hence, an even simpler model consisting of an ideal switch in parallel to an MOV as used in [2] is sufficient. The ideal switch has to be controlled to open after tripping and all expected delays.

In Fig. 9, the breaker current and all path currents are shown for an active resonant breaker. The fault current still looks triangular, but the currents in the commutation and energy absorption path oscillate in the commutation process. These oscillations strongly depend on the spark gap's di/dt capabilities. This, and its modelling should be analyzed in future work.

The commutation from main to commutation path for the ABB breaker with and without LCS is depicted in Fig. 10. To make both models comparable, the assumptions regarding the semiconductors and the stray inductance for active arcing are applied to the ABB breaker with LCS as well. Without LCS, the arc voltage increases slowly at first and even more, when the current commutates out of the main path. With LCS, a counter-voltage is inserted directly, which leads to faster commutation. The commutation time needed with LCS is $10\,\mu\mathrm{s}$, whereas $250\,\mu\mathrm{s}$ was reported in [10]. The values deviate, because we neglected the snubbers. The commutation without LCS takes $100\,\mu\mathrm{s}$, whereas $2.4\,\mathrm{ms}$ was reported in [11]. This is a substantial deviation and there are several reasons for this. Firstly, in that paper a $40.5\,\mathrm{kV}$ SF6 breaker was used, so that the black-box model parameters would differ from what we used. Secondly, the actual stray inductance in their test circuit is most likely larger than what we assumed, because the experimental space was relatively small. Thirdly, the conditions in their test circuit are different from our simulation test grid. This can be seen in their results that the commutation takes place when the slowly resonating test current is at its peak and the current is almost constant throughout the commutation. A simulation showed that the snubbers do not have a large impact without LCS.

5 Summary

Simplified modelling of HVDC breakers for HVDC grid simulations was described in this paper. The results showed that from a grid perspective the fault current waveform looks like a triangle and the breaker voltage depends on the time when the MOV starts to conduct and the fault current level at that time. An ideal switch in parallel with an MOV suffices for grid simulations. However, the proposed models are still useful to estimate interruption times or to roughly dimension a breaker before going to detailed models. If a breaker contains capacitors or inductors, it is possible that these interact with the grid and trigger resonances. Thus, the models can be used in HVDC grid stability studies.

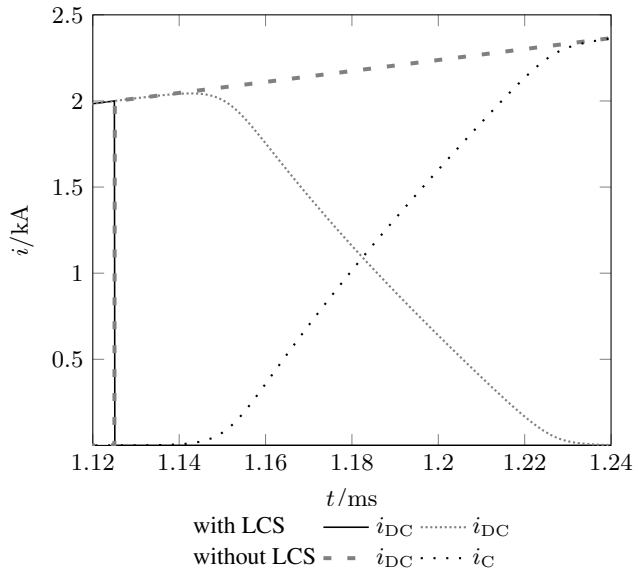

Fig. 10: Comparison commutation from main to commutation path for ABB breaker with and without LCS

If the currents in the different breaker paths need to depicted more accurately, snubbers have to be considered. Nevertheless, if only the interruption time is of interest, an estimated delay can be used in the breaker control instead. Regarding future activities, we think that accurate models of active resonant breakers should be developed with more focus on the spark gap.

References

[1] Working Group B4.52, "HVDC Grid Feasibility Study," CIGRÉ, Tech. Rep., Apr. 2013.

[2] W. Leterme, N. Ahmed, J. Beerten, L. Ängquist, D. Van Hertem, and S. Norrga, "A new HVDC grid test system for HVDC grid dynamics and protection studies in EMT-type software," in *11th IET International Conference on AC and DC Power Transmission*, Birmingham, Feb. 2015, pp. 1–7.

[3] C. M. Franck, "HVDC Circuit Breakers: A Review Identifying Future Research Needs," *IEEE Transactions on Power Delivery*, vol. 26, no. 2, pp. 998–1007, Apr. 2011.

[4] A. Greenwood and T. Lee, "Theory and Application of the Commutation Principle for HVDC Circuit Breakers," *IEEE Transactions on Power Apparatus and Systems*, vol. PAS-91, no. 4, pp. 1570–1574, Jul. 1972.

[5] K. Tahata, S. El Oukaili, K. Kamei, D. Yoshida, Y. Kono, R. Yamamoto, and H. Ito, "HVDC circuit breakers for HVDC grid applications," in *11th IET International Conference on AC and DC Power Transmission*, Feb. 2015, pp. 1–9.

[6] B. C. Kim, Y. H. Chung, H. D. Hwang, and H. S. Mok, "Comparison of inverse current injecting HVDC curcuit breaker," in *3rd International Conference on Electric Power Equipment - Switching Technology (ICEPE-ST)*, Busan, Oct. 2015, pp. 501–505.

[7] Y. Wang and R. Marquardt, "Performance of a new fast switching DC-Breaker for meshed HVDC-Grids," in *17th European Conference on Power Electronics and Applications (EPE'15-ECCE Europe)*, Geneva, Sep. 2015, pp. 1–9.

[8] J. Häfner and B. Jacobson, "Proactive Hybrid HVDC Breakers - A key innovation for reliable HVDC grids," in *CIGRÉ Symposium*, vol. 264, Bologna, Sep. 2011.

[9] P. Skarby and U. Steiger, "An Ultra-fast Disconnecting Switch for a Hybrid HVDC Breaker – a technical breakthrough," in *CIGRÉ Canada Conference*, vol. 265, Calgary, Sep. 2013.

[10] A. Hassanpoor, J. Häfner, and B. Jacobson, "Technical Assessment of Load Commutation Switch in Hybrid HVDC Breaker," in *International Power Electronics Conference (IPEC-Hiroshima 2014 ECCE-ASIA)*, Hiroshima, May 2014, pp. 3667–3673.

[11] W. Wen, Y. Huang, Y. Sun, J. Wu, M. Al-Dweikat, and W. Liu, "Research on Current Commutation Measures for Hybrid DC Circuit Breakers," *IEEE Transactions on Power Delivery*, vol. 31, no. 4, pp. 1456–1463, Aug. 2016.

[12] C. Davidson, R. Whitehouse, C. Barker, J.-P. Dupraz, and W. Grieshaber, "A new ultra-fast HVDC Circuit breaker for meshed DC networks," in *11th IET International Conference on AC and DC Power Transmission*, Feb. 2015, pp. 1–7.

[13] W. Zhou, X. Wei, S. Zhang, G. Tang, Z. He, J. Zheng, Y. Dan, and C. Gao, "Development and test of a 200kV full-bridge based hybrid HVDC breaker," in *17th European Conference on Power Electronics and Applications (EPE'15 ECCE-Europe)*, Sep. 2015, pp. 1–7.

[14] M. T. Thompson, "Inductance Calculation Techniques - Part 2: Approximations and Handbook Methods," *Power Control and Intelligent Motion*, Dec. 1999.

[15] R. P. P. Smeets and V. Kertész, "Application of a Validated AC Black-Box Arc Model to DC Current Interruption," in *2nd International Conference on Electric Power Equipment - Switching Technology (ICEPE-ST)*, Matsue, Oct. 2013, pp. 1–4.

[16] ——, "A new arc parameter database for characterization of short-line fault interruption capability of high-voltage circuit breakers," in *CIGRÉ Session*, Paris, Aug. 2006.